CERN-TH.6510/92

One-loop corrections to three vector boson vertices in the Standard Model

E.N.Argyres[1,2], G.Katsilieris[2], A.B.Lahanas[3],

C.G.Papadopoulos[1] and V.C.Spanos[2]

Abstract

We study the one-loop corrections to the three boson vertices γW^+W^- and ZW^+W^-, and we present expressions for the dipole $\Delta\kappa_V$ and quadrupole ΔQ_V form factors as a function of Q^2, m_{top} and m_{Higgs}, where Q^μ is half of the 4-momentum carried by the neutral bosons. We also discuss the relevance of our results to future experiments, where reactions of the type $f_R\bar{f}_R \to W^+W^-$ at high Q^2 will be analysed and we show that (I) it might be possible, given a good experimental sensitivity, to extract valuable informations for the mass of the top quark and (II) that any measured value of $\Delta\kappa_V$ above 10^{-2} will be a signal of new physics.

CERN-TH.6510/92
May 1992

[1]CERN.TH-Division,CH-1211,Geneva 23, Switzerland
[2]NRCPS.'Democritos',Aghia Paraskevi GR-15310.Athens.Greece
[3]University of Athens, Physics Department .GR-15771.Athens,Greece

1 Introduction.

One of the most crucial, precise and untested predictions of the standard model of electroweak interactions is the magnitude and structure of the three-boson couplings. These couplings are a direct consequence of the gauge symmetry and specifically of the non-abelian nature of the underlying $SU(2)$ Lie algebra. Physically they are related to the static properties of the massive gauge bosons $W^{\pm}$, namely, the magnetic dipole μ_W and the electric quadrupole Q_W moments.

In order to test the structure of the 3-boson coupling one has to parametrize it in the most general way, compare it with the experimental data and thus verify or rule out the Standard Model predictions. The most general parametrization leads to 9 form factors [1] among which κ_γ and λ_γ are the most important, compatible with C-, P- and T- invariance. They are related to the static quantities μ_W and Q_W

$$\begin{aligned} \mu_W &= \frac{e}{2M_W}(1+\kappa_\gamma+\lambda_\gamma) \\ Q_W &= -\frac{e}{M_W^2}(\kappa_\gamma-\lambda_\gamma) \end{aligned} \tag{1}$$

The Standard model at tree order predicts $\kappa_\gamma = 1$ and $\lambda_\gamma = 0$.

So far there are no severe experimental bounds on κ and λ. The most recent analysis on the observed rate of $W\gamma$ events in $p\bar{p}$ collisions at $\sqrt{s} = 0.63, 1.8$TeV has yielded the following bounds at 95% CL.[2]

$$\begin{aligned} -3.5 &\leq \kappa_\gamma \leq 5.9 \\ -3.6 &\leq \lambda_\gamma \leq 3.5 \end{aligned} \tag{2}$$

However, forthcoming experiments, LEPII, NLC, LHC, SSC and HERA, may measure κ and λ with higher accuracy, of the order of 10^{-2} to 10^{-3}[3].

The precision achievable by future experiments will provide the possibility to test not only the tree order predictions of the Standard Model , but also the radiative corrections, namely the one-loop 3-boson couplings. The value of this test might be of more than academic interest, if one considers the dependence of the one-loop result on the Standard Model unknown parameters, like the top-quark and the Higgs mass, which can then be more or less constrained by the measurement of 3-boson couplings.

In this paper we study the one-loop 3-boson vertices in the framework of the Standard Model and discuss the sensitivity of the results on the top-quark and Higgs mass. The paper is organized as follows. In section 2 we describe the stucture of the 3-boson vertex and the way κ and λ are extracted from the one-loop calculations. In subsections 2.1, 2.2 and 2.3 we present the results for gauge boson graph contributions, Higgs and fermions respectively. Finally, in section 3, we discuss our results and especially their sensitivity to the top mass parameter.

2 Three boson vertices at one loop

The most general W^+W^-V vertex, where V stands for Z^0 and γ, with the W's on mass-shell and V an off-shell gauge boson, can be written as follows [4] (see fig.1 for notation),

$$\begin{aligned} \Gamma^V_{\mu\alpha\beta} &= -ig_{WV}\Big(f[2g_{\alpha\beta}\Delta_\mu + 4(g_{\alpha\mu}Q_\beta - g_{\beta\mu}Q_\alpha)] \\ &+ 2\Delta\kappa_V(g_{\alpha\mu}Q_\beta - g_{\beta\mu}Q_\alpha) \\ &+ 4\frac{\Delta Q_V}{M_W^2}(\Delta_\mu Q_\alpha Q_\beta - Q^2 g_{\alpha\beta}\Delta_\mu)\Big) + \ldots \end{aligned} \tag{3}$$

where

$$\begin{aligned} g_{WV} &= e \quad g_{WZ} = e\cot\theta_W \\ \Delta\kappa_V &= \kappa_V + \lambda_V - 1 \\ \Delta Q_V &= -\lambda_V \end{aligned} \tag{4}$$

and the ellipses denote C or P violating terms, as well as terms proportional to Q^μ, which we do not present since we are interested in cases where the neutral bosons couple to massless fermions. The lowest order vertex in the Standard Model corresponds to $f = 1$, $\Delta\kappa_V = \Delta Q_V = 0$. At one loop the divergence of f will be absorbed by the charge renormalization.

It is clear from Eq.(3) that in order to extract the one-loop contribution to $\Delta\kappa_V$ and ΔQ_V we need to calculate only the factors $a_i(Q^2)$ $(i = 1, 2, 3)$, where

$$\begin{aligned} \Gamma^V_{\mu\alpha\beta}(1-\text{loop}) &= -ig_{WV}\Big(a_1^V(Q^2)\Delta_\mu g_{\alpha\beta} \\ &+ a_2^V(Q^2)(g_{\alpha\mu}Q_\beta - g_{\beta\mu}Q_\alpha) \\ &+ a_3^V(Q^2)\Delta_\mu Q_\alpha Q_\beta\Big) \end{aligned} \tag{5}$$

then the values of $\Delta\kappa_V$ and ΔQ_V are given by

$$\Delta\kappa_V = \frac{1}{2}(a_2^V(Q^2) - 2a_1^V(Q^2) - 2Q^2 a_3^V(Q^2)) \tag{6}$$

$$\Delta Q_V = \frac{M_W^2}{4}a_3^V(Q^2) \tag{7}$$

Notice that $\Delta\kappa_V$, ΔQ_V are both finite, whereas a_1^V, a_2^V are separately divergent.

There are three kinds of graphs contributing to $\Gamma^V_{\mu\alpha\beta}$, namely

1. Gauge boson graphs.(In this class of graphs we also include the ghost and Goldstone boson loops associated with the gauge fixing of the local symmetry.)

2. Higgs scalar loop graphs.

3. Fermion loop graphs.

We will now proceed to discuss each of these contributions separately.

2.1 Gauge Boson Graphs.

For our calculations we find it convenient to work in the 't Hooft- Feynman gauge. Thus, unlike the unitary gauge, one has to consider Goldstone boson and ghost contributions. All relevant graphs are shown in fig.2a.

The most difficult graph to calculate is that of fig.2a(a), in which three gauge bosons meet in all three vertices. This calculation is presented in the Appendix.

The contributions of the graph of fig.2a to the $\Delta\kappa^{VWW}(Q^2)$ and $\Delta Q^{VWW}(Q^2)$ form factors with V either γ or Z are as follows:

1. Graph 2a(a)

$$\Delta\kappa^{VWW}(Q^2) = f_a\left\{\frac{G_F M_W^2}{4\pi^2\sqrt{2}}\frac{1}{R}\int_0^1 dtt\int_0^1 da\frac{\mathcal{J}}{L^2}+\frac{\alpha}{8\pi}\int_0^1 dtt\int_0^1 da\frac{\mathcal{J}_\gamma}{L_\gamma^2}\right\} \quad (8)$$

$$\Delta Q^{VWW}(Q^2) = f_a\left\{\frac{G_F M_W^2}{4\pi^2\sqrt{2}}\frac{36}{R}\int_0^1 dtt^3(1-t)\int_0^1 da\frac{a(1-a)}{L^2} + \frac{\alpha}{8\pi}36\int_0^1 dtt^3(1-t)\int_0^1 da\frac{a(1-a)}{L_\gamma^2}\right\} \quad (9)$$

2. Graphs 2a(b)+2a(c)

$$\Delta\kappa^{VWW}(Q^2) = f_b\left\{\frac{G_F M_W^2}{4\pi^2\sqrt{2}}\frac{3(1-R)}{R}\int_0^1 dtt^2\int_0^1 da\frac{1}{L^2} + \frac{\alpha}{8\pi}3\int_0^1 dtt^2\int_0^1 da\frac{1}{L_\gamma^2}\right\} \quad (10)$$

$$\Delta Q^{VWW}(Q^2) = 0 \quad (11)$$

3. Graph 2a(d)

$$\Delta\kappa^{VWW}(Q^2) = -f_c\left\{\frac{G_F M_W^2}{4\pi^2\sqrt{2}}\frac{4(1-R)^2}{R}\int_0^1 dtt(1-t)\int_0^1 da\frac{1}{L^2} + \frac{\alpha}{8\pi}4\int_0^1 dtt(1-t)\int_0^1 da\frac{1}{L_\gamma^2}\right\} \quad (12)$$

$$\Delta Q^{VWW}(Q^2) = 0 \quad (13)$$

4. Graph 2a(e)

$$\Delta\kappa^{VWW}(Q^2) = f_e\frac{G_F M_W^2}{4\pi^2\sqrt{2}}\int_0^1 dt\int_0^1 dat^2(1-t) [-8\frac{Q^2}{M_W^2}ta(1-a)-2t+R]\frac{1}{L^2} \quad (14)$$

$$\Delta Q^{VWW}(Q^2) = f_e\frac{G_F M_W^2}{4\pi^2\sqrt{2}}4\int_0^1 dtt^3(1-t)\int_0^1 da\frac{a(1-a)}{L^2} \quad (15)$$

5. Graphs 2a(f) to 2a(j)

$$\Delta\kappa^{VWW}(Q^2) = f_a\left\{\frac{G_F M_W^2}{4\pi^2\sqrt{2}}[\frac{-3}{R}\int_0^1 dt\frac{2t^3-(8+R)t^2+4tR}{t^2+R(1-t)} + 9\int_0^1 dtln(1-\frac{4Q^2}{M_W^2}t(1-t))] + \frac{21\alpha}{8\pi}\right\} \quad (16)$$

$$\Delta Q^{VWW}(Q^2) = 0 \quad (17)$$

6. Graph 2a(k)

$$\Delta\kappa^{VWW}(Q^2) = f_a\left\{\frac{G_F M_W^2}{4\pi^2\sqrt{2}}\frac{1}{R}\int_0^1 dt\int_0^1 dat^2(1-t) [8\frac{Q^2}{M_W^2}ta(1-a)+2t-R]\frac{1}{L^2} + \frac{\alpha}{8\pi}\int_0^1 dt\int_0^1 da\frac{t^2(1-t)[8\frac{Q^2}{M_W^2}ta(1-a)+2t]}{L_\gamma^2}\right\} \quad (18)$$

$$\Delta Q^{VWW}(Q^2) = -f_a\left\{\frac{G_F M_W^2}{4\pi^2\sqrt{2}}\frac{4}{R}\int_0^1 dtt^3(1-t)\int_0^1 da\frac{a(1-a)}{L^2} + \frac{\alpha}{8\pi}4\int_0^1 dtt^3(1-t)\int_0^1 da\frac{a(1-a)}{L_\gamma^2}\right\} \quad (19)$$

In the expressions above $R \equiv \frac{M_Z^2}{M_W^2} = \frac{1}{\cos^2\theta_W}$ and the functions $\mathcal{J}, L, \mathcal{J}_\gamma$ and L_γ are defined as follows:

$$\mathcal{J} = \frac{Q^2}{M_W^2}(24t^2(-5+7t)a(1-a)-2t^2(1-2a)^2-(10t^2-28t+8)) + 5R(1-t)(4-3t)-(6t^3-4t^2+15t-4) \quad (20)$$

$$\mathcal{J}_\gamma = [\text{as } \mathcal{J} \text{ with } R=0] \quad (21)$$

$$L^2 = -\frac{4Q^2}{M_W^2}t^2a(1-a)+t^2+R(1-t) \quad (22)$$

$$L_\gamma^2 = [\text{as } L^2 \text{ with } R=0] \quad (23)$$

The graphs (f) to (j) of fig.2a have ultraviolet $\frac{1}{\epsilon}$ singularities which, however, cancel in the sum. The prefactors appearing in the expressions are given by

$$V = \gamma \quad : \quad f_a = f_b = f_c = 1 \tag{24}$$

$$V = Z \quad : \quad f_a = 1, \quad f_b = -(R-1), \quad f_c = \frac{1}{2}(2-R) \tag{25}$$

Putting $Q^2 = 0$ and summing up the contributions of all graphs of fig. 2a(a) to 2a(k) we recover exactly the results of reference [5] for the corresponding quantities. In their calculations they used the unitary gauge. This serves as a check of the correctness of our results.

At zero momentum transfer some of the graphs, namely 2a(a) and 2a(d), exhibit infrared singularities in $\Delta\kappa^{VWW}(Q^2)$ for $V = \gamma$ which however cancel in the sum. At this point we should remark that for $Q^2 \neq 0$ the graph 2a(a) has an infrared singularity due to the photon exchange which is not cancelled by anything else. This arises from the last term of β_1 multiplying $\frac{Q^2}{M_W^2}$ and is given by

$$-\frac{\alpha}{\pi}\frac{Q^2}{M_W^2}\int_0^1 dtt\int_0^1 da\frac{1}{[-\frac{4Q^2}{M_W^2}t^2a(1-a)+t^2+\frac{m_\gamma^2}{M_W^2}(1-t)]} \tag{26}$$

where we have introduced a small photon mass m_γ for the exchanged photon. In the limit $m_\gamma \to 0$ this crearly exhibits an infrared singularity proportional to $log(\frac{m_\gamma^2}{Q^2})$. It is well known that these singularities are cancelled in real physical processes if one takes into account the soft photon emission. In principle, the cancellation of infrared singularities introduces a finite part which depends on the process under consideration. This does not, however, invalidate the calculation of the $\Delta\kappa_V$ form factors since when right handed fermions are involved, for instance in the process $f\bar{f} \to W^+W^-$, the main (s-channel) contribution of these couplings is proportional to

$$\Delta\kappa_\gamma - \frac{s}{s-M_Z^2}\Delta\kappa_Z = \Delta\kappa_\gamma - \Delta\kappa_Z + O(\frac{M_Z^2}{s}) \tag{27}$$

(see for instance eqn.(7a) of reference [6]) where $s = 4Q^2$ and the difference $\Delta\kappa_\gamma - \Delta\kappa_Z$ is free of infrared singularities, and thus independent of the specific process under consideration.

2.2 Higgs Boson Graphs

All graphs with at least a physical Higgs H circulating in the loop are shown in fig.2b. Notice that for the vertex ZW^+W^- the additional graphs fig.2b (d_1),(d_2), not present in the γW^+W^- case, appear due to the existence of the couplings $Z\phi_2 H$, ZZH. The graphs fig.2b(b),(c) yield vanishing contributions to $\Delta\kappa(Q^2)$, $\Delta Q(Q^2)$.

The total contribution of the graphs displayed in fig.2b to the photon form factors is given below:

$$\begin{aligned}\Delta\kappa^{\gamma WW}(Q^2) &= \frac{G_F M_W^2}{4\pi^2\sqrt{2}}\int_0^1 dt\int_0^1 da(2t^4-(\mu^2+2)t^3+(\mu^2+4)t^2 \\ &- \frac{8Q^2}{M_W^2}a(1-a)(1-t)t^3)\frac{1}{L_H^2}\end{aligned} \tag{28}$$

$$\Delta Q^{\gamma WW}(Q^2) = \frac{G_F M_W^2}{4\pi^2\sqrt{2}}\int_0^1 dt\int_0^1 da\frac{4t^3(1-t)a(1-a)}{L_H^2} \tag{29}$$

In these expressions $\mu^2 \equiv \frac{M_H^2}{M_W^2}$ where M_H is the mass of the Higgs and L_H^2 is given by

$$L_H^2 = t^2 + \mu^2(1-t) - \frac{4Q^2}{M_W^2}t^2a(1-a) \tag{30}$$

For the ZW^+W^- form factors we have

$$\begin{aligned}\Delta\kappa^{ZWW}(Q^2) &= \frac{G_F M_W^2}{4\pi^2\sqrt{2}}\Big\{\frac{1}{2}\int_0^1 dt\int_0^1 da[(4-2R)t^4-(\mu^2+2)(2-R)t^3 \\ &+ (8-2R-R\mu^2+2\mu^2)t^2 - \frac{8Q^2}{M_W^2}(2-R)a(1-a)(1-t)t^3]\frac{1}{L_H^2} \\ &+ R\int_0^1 dt\int_0^1 da(t^2(t-1)[2(t-1)+(R-\mu^2)a+\mu^2 \\ &+ \frac{8Q^2}{M_W^2}ta(1-a)] - 6at^2)\frac{1}{\hat{L}_H^2} \\ &+ R(R-1)\int_0^1 dt\int_0^1 da\frac{2at^2}{\hat{L}_H^2}\Big\}\end{aligned} \tag{31}$$

$$\begin{aligned}\Delta Q^{ZWW}(Q^2) &= \frac{G_F M_W^2}{4\pi^2\sqrt{2}}\Big\{\frac{(2-R)}{2}\int_0^1 dt\int_0^1 da\frac{4t^3(1-t)(1-a)a}{L_H^2} \\ &+ R\int_0^1 dt\int_0^1 da\frac{4at^3(1-t)(1-a)}{\hat{L}_H^2}\Big\}\end{aligned} \tag{32}$$

In these expressions $R \equiv \frac{M_Z^2}{M_W^2}$, L_H^2 is as given before while the denominator $\hat{L}_H^2$ associated with the graphs depicted in fig.2b(d_1),(d_2) is given by

$$\hat{L}_H^2 = (t-1)^2 + Rat + \mu^2 t(1-a) - \frac{4Q^2}{M_W^2}t^2a(1-a) \tag{33}$$

The γW^+W^- form factors for $Q^2 = 0$ yield exactly the results of reference [5].

2.3 Fermion Graphs

The fermionic contribution to the dipole and quadrupole form factors stem from triangle graphs of the type shown in figure 2c, where a summation over all possible fermion loops is understood. For the calculations we write the relevant interaction Lagrangian as follows:

$$L = -\frac{g}{\sqrt{2}}[W_\mu^- \bar{f'}_L \gamma^\mu f_L + (h.c)] + V_\mu[g_L^f \bar{f}_L \gamma^\mu f_L + g_R^f \bar{f}_R \gamma^\mu f_R] \tag{34}$$

In the above expression V_μ stands for either a photon or a Z- boson while g_L^f, g_R^f are the left and right handed couplings. The result we get from the graphs of fig.2c is

$$\begin{aligned}\Delta\kappa^{VWW}(Q^2) &= c_V \frac{G_F M_W^2}{4\pi^2\sqrt{2}} C_f \Big\{(-\frac{g_L^f}{\epsilon}) \int_0^1 dt \int_0^1 da \Big(t^4 + t^3(-1+\epsilon-\Delta) \\ &+ t^2(\Delta-\epsilon) + \frac{4Q^2}{M_W^2} t^3(7t-6)a(1-a)\Big)\frac{1}{L_f^2} \\ &+ (-\frac{g_R^f}{\epsilon})\Delta \int_0^1 dt \int_0^1 da \frac{t^2}{L_f^2}\Big\} \end{aligned} \tag{35}$$

$$\Delta Q^{VWW}(Q^2) = c_V \frac{G_F M_W^2}{4\pi^2\sqrt{2}} C_f \Big\{8(-\frac{g_L^f}{\epsilon}) \int_0^1 dt \int_0^1 da \frac{t^3(1-t)(1-a)a}{L_f^2}\Big\} \tag{36}$$

where $\epsilon \equiv \frac{m_{f'}^2}{M_W^2}$ and $\Delta \equiv \frac{m_f^2}{M_W^2}$, while L_f^2 is given by

$$L_f^2 = t^2(1 - \frac{4Q^2}{M_W^2}a(1-a)) - t(1+\epsilon-\Delta) + \epsilon \tag{37}$$

The prefactor C_f is the colour factor equal to 3 for quark loops and to 1 for lepton loops, while $c_\gamma = 1$, $c_Z = tan\theta_W$. The left and right couplings of the fermions to γ and Z are given below:

$$V = \gamma \quad : \quad (-\frac{g_L^f}{\epsilon}) = (-\frac{g_R^f}{\epsilon}) = Q_f \tag{38}$$

$$\begin{aligned} V = Z \quad : \quad (-\frac{g_L^f}{\epsilon}) &= \frac{1}{sin\theta_W cos\theta_W}(t_3^f - Q_f sin^2\theta_W) \\ (-\frac{g_R^f}{\epsilon}) &= \frac{1}{sin\theta_W cos\theta_W}(-Q_f sin^2\theta_W) \end{aligned} \tag{39}$$

To specify our notation we give the charge (Q_f) and the weak isospin (t_3^f) for the various fermions in table 1.

At zero momentum transfer ($Q^2 = 0$) and limiting ourselves to the third family contribution our results for $\Delta\kappa^{\gamma WW}(Q^2)$ and $\Delta Q^{\gamma WW}(Q^2)$ coincide with those given

Fermions	Q_f	t_3^f
u, c, t	$\frac{2}{3}$	$\frac{1}{2}$
d, s, b	$-\frac{1}{3}$	$-\frac{1}{2}$
$\nu_{e,\mu,\tau}$	0	$\frac{1}{2}$
e, μ, τ	-1	$-\frac{1}{2}$

Table 1: Fermion charges and weak isospins.

in reference [7]. For our numerical calculations the values of the quark masses of the first two generations as well as those of all leptons are taken equal to zero. In this approximation the contribution of the first two fermion families vanishes owing to the triangle anomaly cancellation relation $\sum_f t_3^2(f)Q_f = 0$, which holds separately for each family. In view of this only the third family contribution need to be taken into account.

A subtlety arises at $Q^2 = 0$ when the masses m_t, m_b of the top and bottom quarks respectively satisfy the relation

$$M_W = m_t \pm m_b \tag{40}$$

Although such top masses are not of practical interest due to the existing experimental bounds on the m_t, it should not pass unnoticed that fermion loops exhibit singularities when Eq.(40) is satisfied. Presumably in a real measurable process such as $e^-W^+ \to e^-W^+$ for instance, see fig.3, these divergences will cancel in the cross section if one takes into account the process $e^-W^+ \to e^-t\bar{b}$ when the invariant mass of the $t\bar{b}$ system is close to M_W or that of $e^-t \to e^-W^+b$ in the case when the Wb mass is close to m_t. This would be the mechanism analogous to that of cancelling the infrared divergences in QED processes. However, lacking the analogue of the Bloch-Nordsieck theorem in this case this is merely a conjecture.

3 Results and conclusions

In order to get numerical estimates of the form factors $\Delta\kappa_V$ and ΔQ_V we perform numerically the double integration over the Feynman parameters t, a. More specifically we take the principal part on the first integration (say da) since there exist simple poles inside the integration region. We have done it by using suitable numerical routines, available in the NAG Fortran Library. Furthermore we have checked these results semi-analytically, i.e. by performing analytically the first integration and then numerically integrating over t, where no pole-structure is present. Finally in one case, Eq.(8), we have checked also the t-integration with the exact analytic re-

sult. Several tests have been made for special values of the parameters in comparison with previous works.

The parameter values we use are:

$$\alpha = \frac{1}{128},\ M_W = 80.6\text{GeV},\ M_Z = 91.1\text{GeV},\ m_b = 5\text{GeV},\ sin^2\theta_W = 0.23 \qquad (41)$$

In fig.4 we present the results for $\Delta\kappa_\gamma$ and ΔQ_γ (solid line) as well as for $\Delta\kappa_\gamma - c(Q^2)\Delta\kappa_Z$ $\Delta Q_\gamma - c(Q^2)\Delta Q_Z$ (dashed line) as a function of $Q = \text{sign}(Q^2)\sqrt{|Q^2|}$, where $c(Q^2) = \frac{4Q^2}{4Q^2 - M_Z^2}$, see Eq.(27). As is well known in processes where real W are produced unitarity may be violated because of the existence of longitudinal polarized W. This is not the case if a non-abelian gauge symmetry is present, since it induces delicate cancelations between different graphs. For instance, in the process $f\bar{f} \to W^+W^-$ with right-handed fermions the cancelation occurs between γ and Z exchange graphs and is based on the relation

$$\kappa_\gamma - \kappa_Z = 0, \qquad \lambda_\gamma - \lambda_Z = 0 \qquad (42)$$

which at tree order in the Standard Model is automatically satisfied. At one loop we see that $\Delta\kappa_\gamma$ is an increasing function of Q^2, and it grows like $log(\frac{Q^2}{M_W^2})$. This essentially reflects the fact that the form factor is not by itself a gauge invariant object in the limit $s \to \infty$, where the local $SU(2)_L \times U(1)_Y$ is restored. Nevertheless, the difference $\Delta\kappa_\gamma - c(Q^2)\Delta\kappa_Z$ vanishes for asymptotic values of Q^2, as unitarity (and gauge symmetry) requires. This means that for asymptotic values of Q^2, the relation Eq.(42) is valid at one loop as well [8]. However, this is not true for intermediate Q^2 values, as we will see below.

In fig.5 we show the fermion contribution for $\Delta\kappa_\gamma$ (solid line: $m_{top} = 150$ GeV, short dashed line: $m_{top} = 200$ GeV) and $\Delta\kappa_\gamma - c(Q^2)\Delta\kappa_Z$ (dashed line: $m_{top} = 150$ GeV, dot-dashed line: $m_{top} = 200$ GeV) and the Higgs contribution for $\Delta\kappa_\gamma$ (solid line: $m_{Higgs} = 100$ GeV, short dashed line: $m_{Higgs} = 150$ GeV) and $\Delta\kappa_\gamma - c(Q^2)\Delta\kappa_Z$ (dashed line: $m_{Higgs} = 100$ GeV, dot-dashed line: $m_{Higgs} = 150$ GeV) as a function of Q. The non-vanishing of the differences of γ and Z form factors is now evident for Q up to 1 TeV. This gives rise to the phenomenon of 'unitarity delay' first discussed in reference [9]. Finally in fig.6 the results for ΔQ_γ and $\Delta Q_\gamma - c(Q^2)\Delta Q_Z$ are presented with the same values of the masses of the top quark and the Higgs scalar as in fig.5.

Although we do not attempt to give a complete answer, we now focus on the question of whether future experiments like LEPII, NLC($\epsilon^+\epsilon^-$, $\sqrt{s}$=500 GeV), LHC and SSC, will be able to test the Standard Model predictions on the three boson couplings. For this we present in fig.7 and 8 the fermion and Higgs contributions for $\Delta\kappa_\gamma$, ΔQ_γ (solid lines) as well as for $\Delta\kappa_\gamma - c(Q^2)\Delta\kappa_Z$ $\Delta Q_\gamma - c(Q^2)\Delta Q_Z$ (dashed lines), as a function of m_{top} and m_{Higgs} respectively, for energies corresponding to $\sqrt{s}$=200 and 500 GeV. Taking into account the limits presented in reference [10] for

LEPII and NLC,

$$\begin{aligned} -0.21\ 10^{-1} &\le \Delta\kappa_\gamma \le 0.22\ 10^{-1} \quad \text{(LEPII)} \\ -0.13\ 10^{-2} &\le \Delta\kappa_\gamma \le 0.14\ 10^{-2} \quad \text{(NLC)} \end{aligned} \qquad (43)$$

we have drawn two solid lines corresponding to the limits for LEPII(NLC) in the first graph of fig.7(8). For LEPII,the Standard Model predictions are below the expected sensitivity[6] and thus no information can be extracted concerning the top mass. Nevertheless, the measurement of $\Delta\kappa_V$, will be very important, since any measured value of it, above the expected sensitivity, will be a straightforward indication of new physics. In contrast for NLC, one can probe top masses of the order of 200-300 GeV, provided that the sensitivity will be of the order of 10^{-3}. This phenomenon should be even stronger in LHC and SSC, but it requires further phenomenological analysis.

The top mass dependence of the one-loop cross section is not of course contained in $\Delta\kappa_V$ [11] only. Nevertheless the m_{top} contribution to f (see Eq.(3)) and to ΔQ_V is negligible compared to the $\Delta\kappa_V$ one. This seems to be also the case in reference [12] where, using longitudinal W, they essentially pick up the $\Delta\kappa_V$ terms. For convenience we give the contributions of gauge boson and Higgs loops which are respectively -5×10^{-5} and 3×10^{-4}, for $\Delta\kappa_\gamma - c(Q^2)\Delta\kappa_Z$ at $\sqrt{s} = 500$GeV. As is evident from fig.8 these contributions are much smaller than the fermionic ones. They are also independent of the top mass.

We conclude that three boson couplings provide a very rich field for both experiment and theory, in order to investigate the microcosm beyond the electroweak scale. Standard Model predictions can be tested, in forthcoming experiments, where large Q^2 will be available and very valuable information on the Standard Model parameters can be extracted. Furthermore, any measurement of these couplings, indicating a value of $\Delta\kappa_V$ above 10^{-2} cannot be explained within the Standard Model and thus offers a possible signal of uew physics.

E.N.A and C.G.P acknowledge support from EEC Program, SC1-CT91-0729.

Appendix.

In the 't Hooft-Feynman gauge the graph of fig.2a when a Z is exchanged between the external W bosons is

$$F_{\mu\alpha\beta} = \int \frac{d^4k}{(2\pi)^4} \frac{V^{\gamma WW}_{\mu\alpha\lambda}(-g^{\lambda\lambda'})V^{ZWW}_{\gamma\beta\delta}(-g^{\delta\delta'})V^{ZWW}_{\gamma\alpha\alpha'}(-g^{\alpha\alpha'})}{[(k-Q)^2-M_W^2][(k+Q)^2-M_W^2][(k-\Delta)^2-M_Z^2]} \qquad (A-1)$$

All kinematics and the flow of momentum are exhibited in fig.1. $V^{\gamma WW}, V^{ZWW}$ are the 3 boson couplings at tree order. The momentum carried by the incomming photon is $2Q$ while the momenta of the W^+, W^- gauge bosons are $p = \Delta - Q$, $p' = -Q - \Delta$.

From Eq.(A-1) we need only extract the coefficients of the tensor structures $g_{\alpha\beta}\Delta_\mu$, $\Delta_\mu Q_\alpha Q_\beta$ and $g_{\alpha\mu}Q_\beta - g_{\beta\mu}Q_\alpha$. For instance if a term $Q_\mu Q_\alpha Q_\beta$ appears in $F_{\mu\alpha\beta}$ it can be ignored, since we are interested in only those terms that contribute to the quadrupole and dipole moments. Their knowledge demands also to know what $g_{\alpha\beta}\Delta_\mu$ coefficient is. The external W gauge bosons are put on their mass shell which means that $Q\cdot\Delta = 0$ and $\Delta^2 + Q^2 = M_W^2$. Besides, the $F_{\mu\alpha\beta}$ vertex will be contracted by ϵ_α^+, ϵ_β^- the polarization vectors of the W gauge bosons. Therefore we have

$$\epsilon_\alpha^+(p)\cdot\Delta^\alpha = \epsilon_\alpha^+(p)\cdot\frac{(p-p')^\alpha}{2} = -\epsilon_\alpha^+(p)\cdot\frac{p'^\alpha}{2} = \epsilon_\alpha^+(p)\cdot Q^\alpha \qquad (A-2)$$

Similarly, $\epsilon_\beta^-(p')\cdot\Delta^\beta = -\epsilon_\beta^-(p')\cdot Q^\beta$. Therefore for the purpose of our calculations $Q_\alpha \to \Delta_\alpha$ and $Q_\beta \to -\Delta_\beta$. This facilitates the calculations a great deal.

The tensor structure of the numerator Eq.(A-1) is

$$\begin{aligned}
T_{\mu\alpha\beta} &= (14-8n)k_\mu k_\alpha k_\beta + 32\Delta_\mu(Q_\beta k_\alpha - Q_\alpha k_\beta) \\
&+ (8n-14)k_\mu(k_\beta Q_\alpha - k_\alpha Q_\beta) + (8n-78)k_\mu Q_\alpha Q_\beta \\
&+ g_{\alpha\beta}[2k_\mu(8Q^2 - 5\Delta^2 - k^2) + 2\Delta_\mu(-2k^2 + 4k\cdot\Delta - 6Q^2)] \\
&+ \Big\{g_{\mu\alpha}[k_\beta(-2k^2 + 2k\cdot(\Delta - Q) - 19Q^2 + \Delta^2 + 24\Delta\cdot Q) \\
&+ Q_\beta(-10k^2 + 2k\cdot(\Delta + 7Q) - 15Q^2 - 3\Delta^2)] + (a\leftrightarrow b, Q\leftrightarrow -Q)\Big\}
\end{aligned}$$

where we have omitted terms not contributing to the quantities we are interested in, and n is the dimension of space-time in a dimensional regularization scheme. With these the $F_{\mu\alpha\beta}$ vertex can be cast in the form

$$F_{\mu\alpha\beta} = (-ieg^2\cos^2\theta_W)\left(\frac{\mu_R}{2\pi}\right)^{4-n} 2\int\frac{d^nk}{(2\pi)^n}\int_0^1 dx\int_0^{1-x} dy\frac{T_{\mu\alpha\beta}}{[k^2 - 2k\cdot l - A^2]^3} \qquad (A-3)$$

In Eq.(A-3) we have introduced the Feynman variables x, y and

$$A^2 = (M_W^2 - Q^2)(x+y) + (M_Z^2 - \Delta^2)(1-x-y) \qquad (A-4)$$

$$l^\mu = Q^\mu(x-y) + \Delta^\mu(1-x-y) \qquad (A-5)$$

Performing the k integration after a lengthy calculation we end up with

$$\begin{aligned}
F_{\mu\alpha\beta} &= -i\frac{\epsilon g\cos^2\theta_W}{16\pi^2}\Big\{[g_{\alpha\beta}\Delta_\mu + 2(g_{\mu\alpha}Q_\beta - g_{\mu\beta}Q_\alpha)\int_0^1 dx\int_0^{1-x} dy\frac{a(Q^2,x,y)}{l^2+A^2} \\
&+ (g_{\mu\alpha}Q_\beta - g_{\mu\beta}Q_\alpha)\int_0^1 dx\int_0^{1-x} dy\frac{b(Q^2,x,y)}{l^2+A^2} \\
&+ (\Delta_\mu Q_\alpha Q_\beta - \Delta_\mu g_{\alpha\beta}Q^2)\int_0^1 dx\int_0^{1-x} dy\frac{c(Q^2,x,y)}{l^2+A^2}\Big\} \qquad (A-6)
\end{aligned}$$

$a(Q^2,x,y)$ is the charge form factor whose explicit form need not be given. By defining new variables as $y = t(1-a)$ and $x = at$ and taking into account Eq.(6) we find

$$\begin{aligned}
F_{\mu\alpha\beta} &= -ie\frac{G_F M_W^2}{2\pi^2\sqrt{2}}\cos^2\theta_W\Big\{(g_{\mu\alpha}Q_\beta - g_{\mu\beta}Q_\alpha)\int_0^1 dtt\int_0^1 da\frac{b(Q^2,x,y)}{L^2} \\
&+ 4(\Delta_\mu Q_\alpha Q_\beta - \Delta_\mu g_{\alpha\beta}Q^2)\frac{18}{M_W^2}\int_0^1 dt\int_0^1 da\frac{t^3(1-t)a(1-a)}{L^2}\Big\} \qquad (A-7)
\end{aligned}$$

where

$$L \equiv -\frac{4Q^2}{M_W^2}t^2a(1-a) + t^2 + \frac{M_Z^2}{M_W^2}(1-t) \qquad (A-8)$$

and

$$\begin{aligned}
b(a,t,Q^2) &= \frac{Q^2}{M_W^2}[24t^2(-5+7t)a(1-a) - 2t^2(1-2a)^2 + (-10t^2+28t-8)] \\
&+ \frac{M_Z^2}{M_W^2}[5(1-t)(4-3t)] + [-6t^3 + 4t^2 - 15t + 4] \qquad (A-9)
\end{aligned}$$

References

[1] K.J.F. Gaemers and G.J.Gounaris. *Z.Phys.* **C1**(1979)259.
K.Hagiwara et *al.*. *Nucl.Phys.* **B282**(1987)253.

[2] UA2 Collaboration. *Phys.Lett* **B227**(1992)194.

[3] U.Baur, D.Zeppenfeld. *Nucl.Phys.* **B325**(1989)253.
U.Baur. D.Zeppenfeld. *Nucl.Phys.* **B308**(1988)127.
E.N.Argyres, O.Korakianitis. C.G.Papadopoulos, *Phys.Lett.* **B259**(1991)195.
E.N.Argyres et *al.*. *Phys.Lett.* **B272**(1991)431.
E.N.Argyres et *al.*. *Phys.Lett.* **B280**(1992)324.

[4] E.N.Argyres. and C.G.Papadopoulos. *Phys.Lett.* **B263**(1991)298.

[5] W.A.Bardeen. R.Gastmans. B.Lautrup. *Nucl.Phys.* **B46**(1972)319.

[6] D.Zeppenfeld. *Phys.Lett.* **B183**(1987)380.

[7] G.Couture and J.N.Ng. *Z.Phys.* **C35**(1987)65.

[8] A.de Rujula. M.B.Gavela. P.Hernandez. E.Masso. 'The self-couplings of vector bosons: does LEP-1 obviate LEP-2?'. CERN-TH.6272/91.
C.P.Burgess and D.London. 'Light spin-one particles imply gauge invariance'. McGill-92/04. 1992.

[9] C.Ahn. B.W.Lynn. M.E.Peskin. S.Selipsky *Nucl.Phys.* **B309**(1988)221.

[10] G.Gounaris et *al.*. 'Trilinear self couplings of vector bosons and their determination in $e^+e^- \to W^+W^-$'. BI-TP 91/40.

[11] M.Bohm et *al.*. *Nucl.Phys.* **B304**(1988)463.

[12] W.Beenakker, 'Resummation of 1PI O(α) fermion loop corrections to $e^+e^- \to W^+W^-$ at high energies'. CERN-TH.6378/92.

Figure Captions

Figure 1. Kinematics of the three boson vertex.

Figure 2. The one loop Feynman graphs for gauge boson (a), Higgs (b) and fermion (c) contributions.

Figure 3. Feynman graphs for $t\bar{b}$ and Wb production.

Figure 4. The Q dependence of $\Delta\kappa_V$ and ΔQ_V for gauge boson contribution, as explained in the text.

Figure 5. The Q dependence of $\Delta\kappa_V$ for fermion and Higgs contributions, as explained in the text.

Figure 6. The Q dependence of ΔQ_V for fermion and Higgs contributions, as explained in the text.

Figure 7. The m_{top} and m_{Higgs} dependence of $\Delta\kappa_V$ and ΔQ_V for $\sqrt{s} = 200$GeV, as explained in the text.

Figure 8. The m_{top} and m_{Higgs} dependence of $\Delta\kappa_V$ and ΔQ_V for $\sqrt{s} = 500$GeV, as explained in the text.

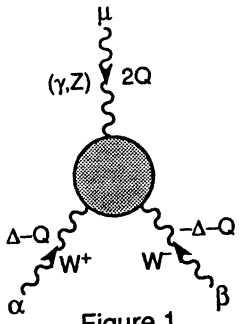

Figure 1

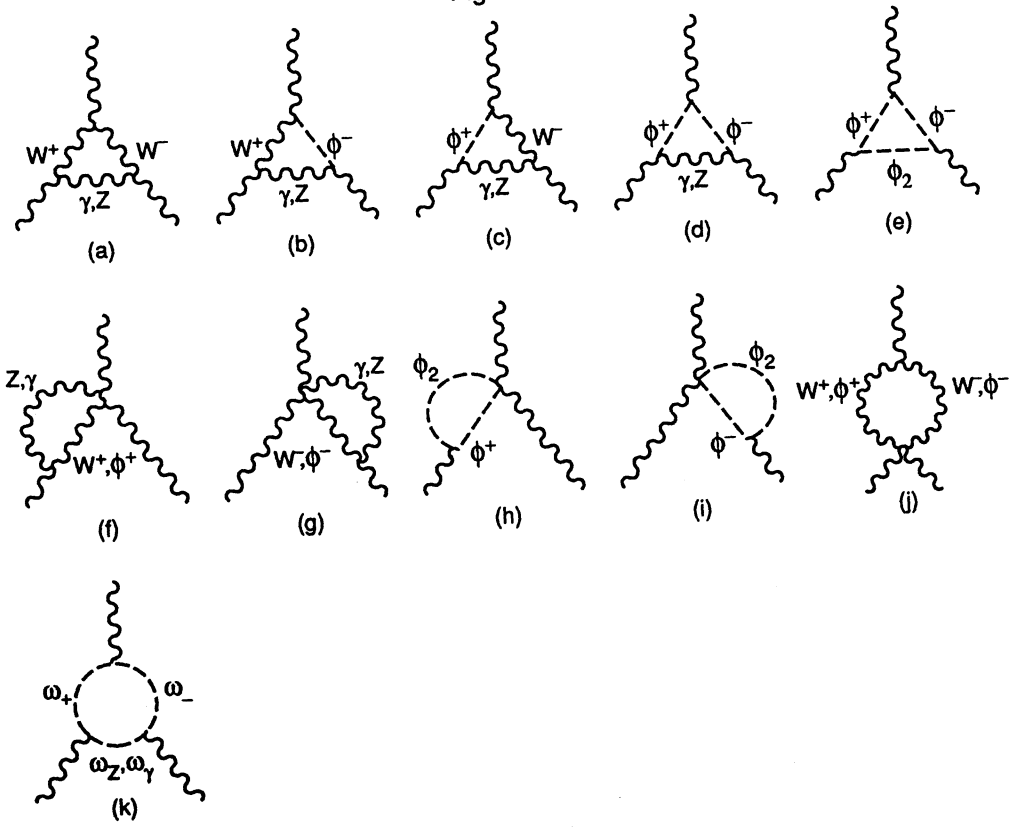

Figure 2a

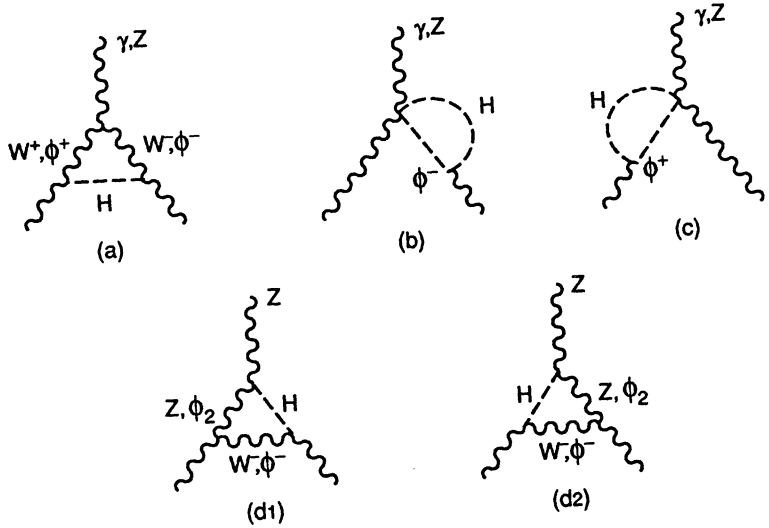

Figure 2b

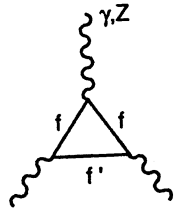

Figure 2c

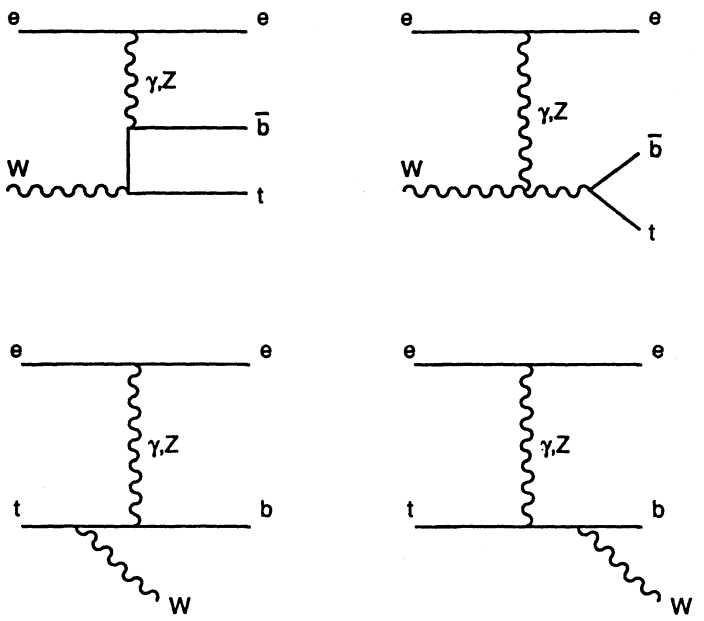

Figure 3

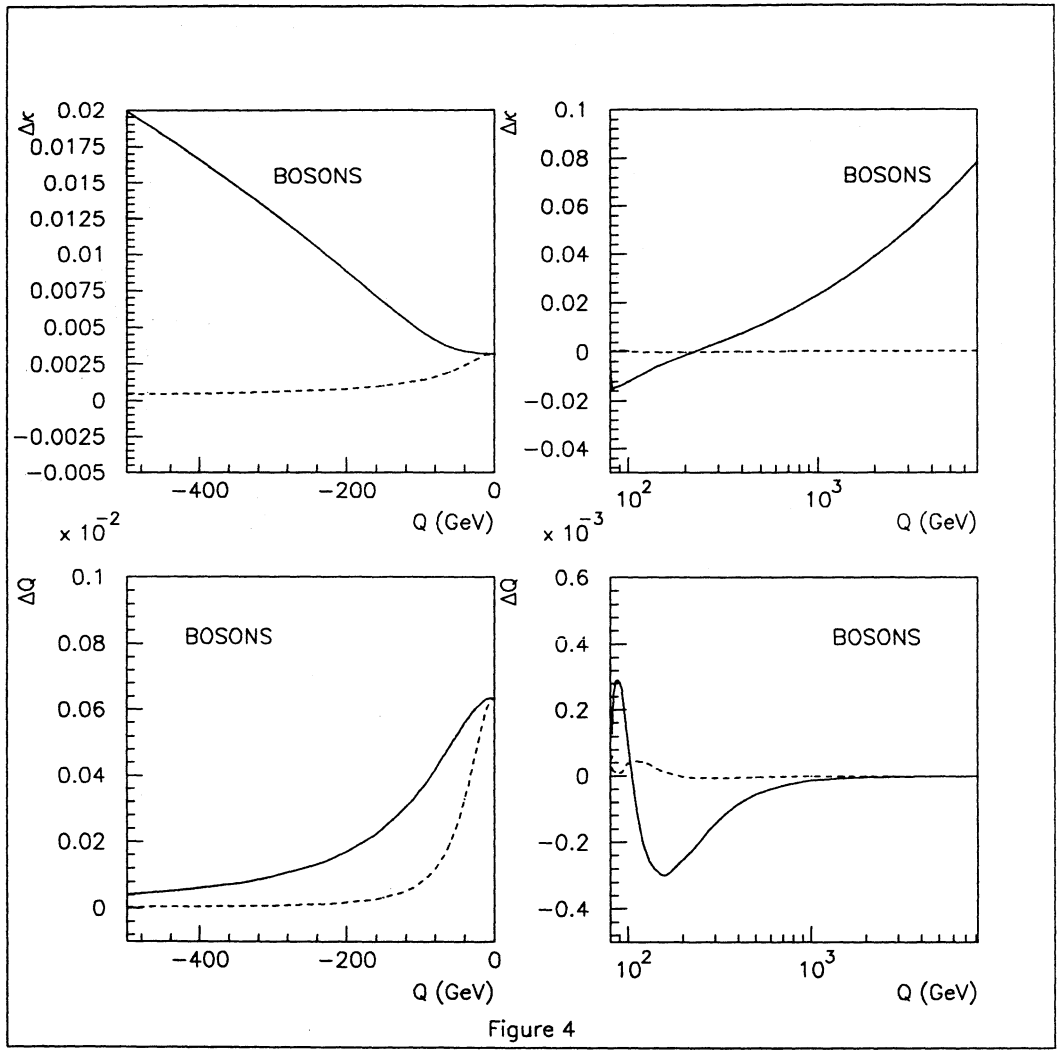

Figure 4

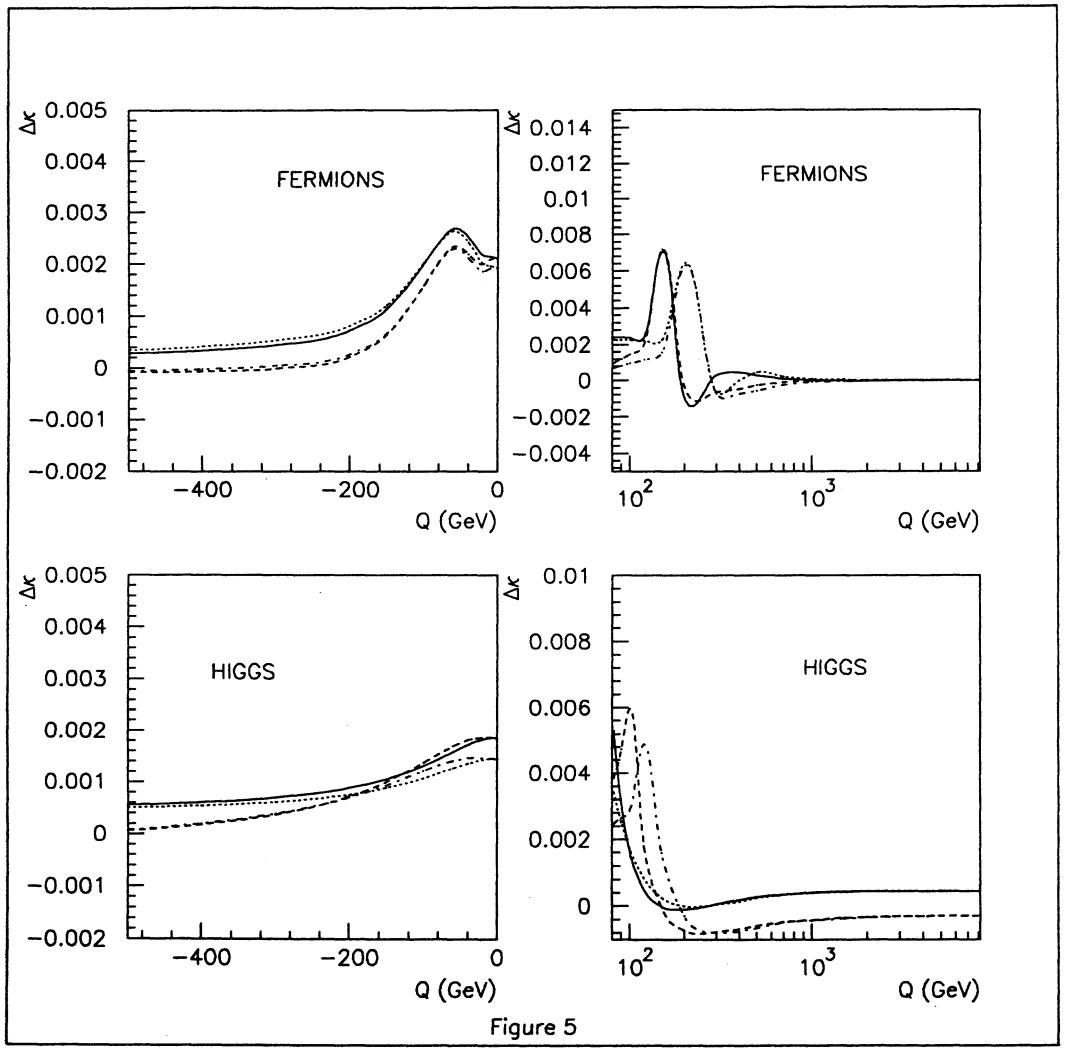

Figure 5

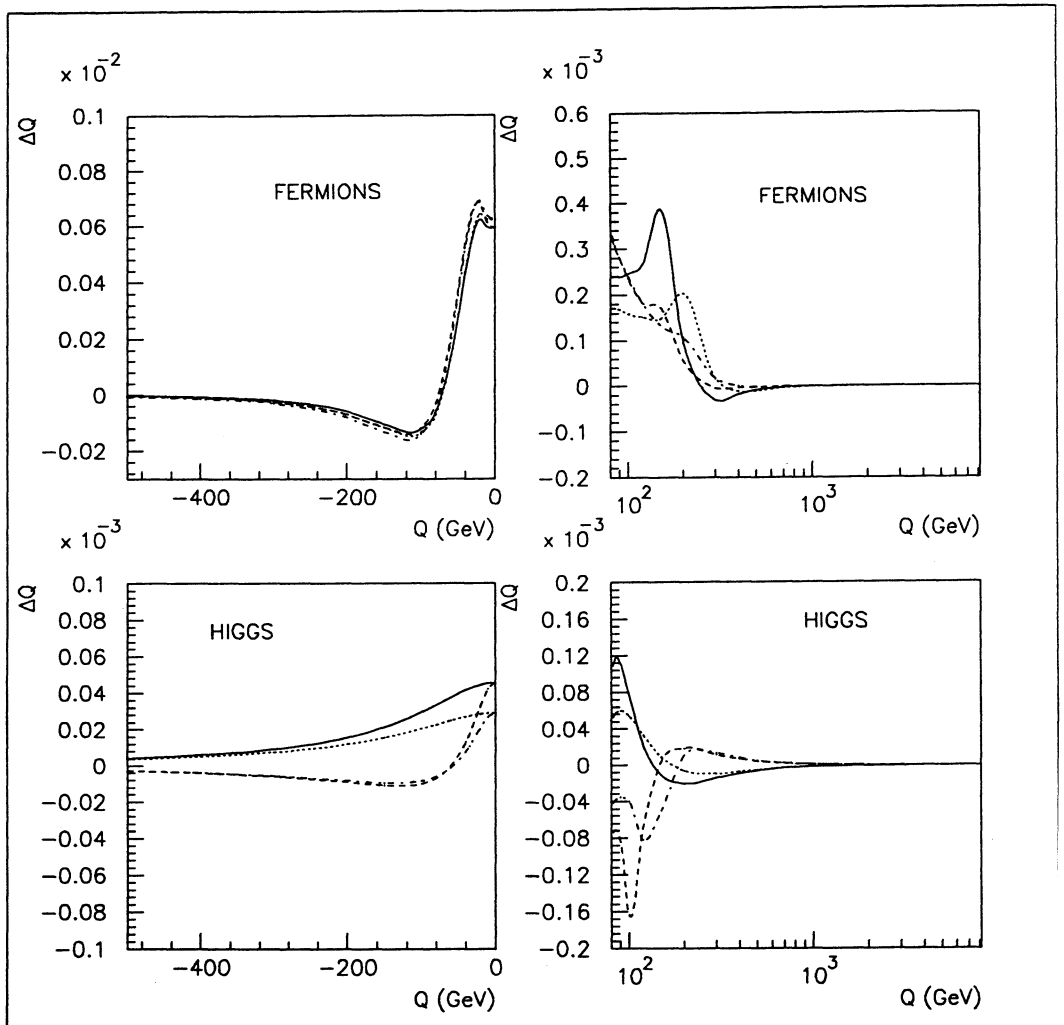

Figure 6

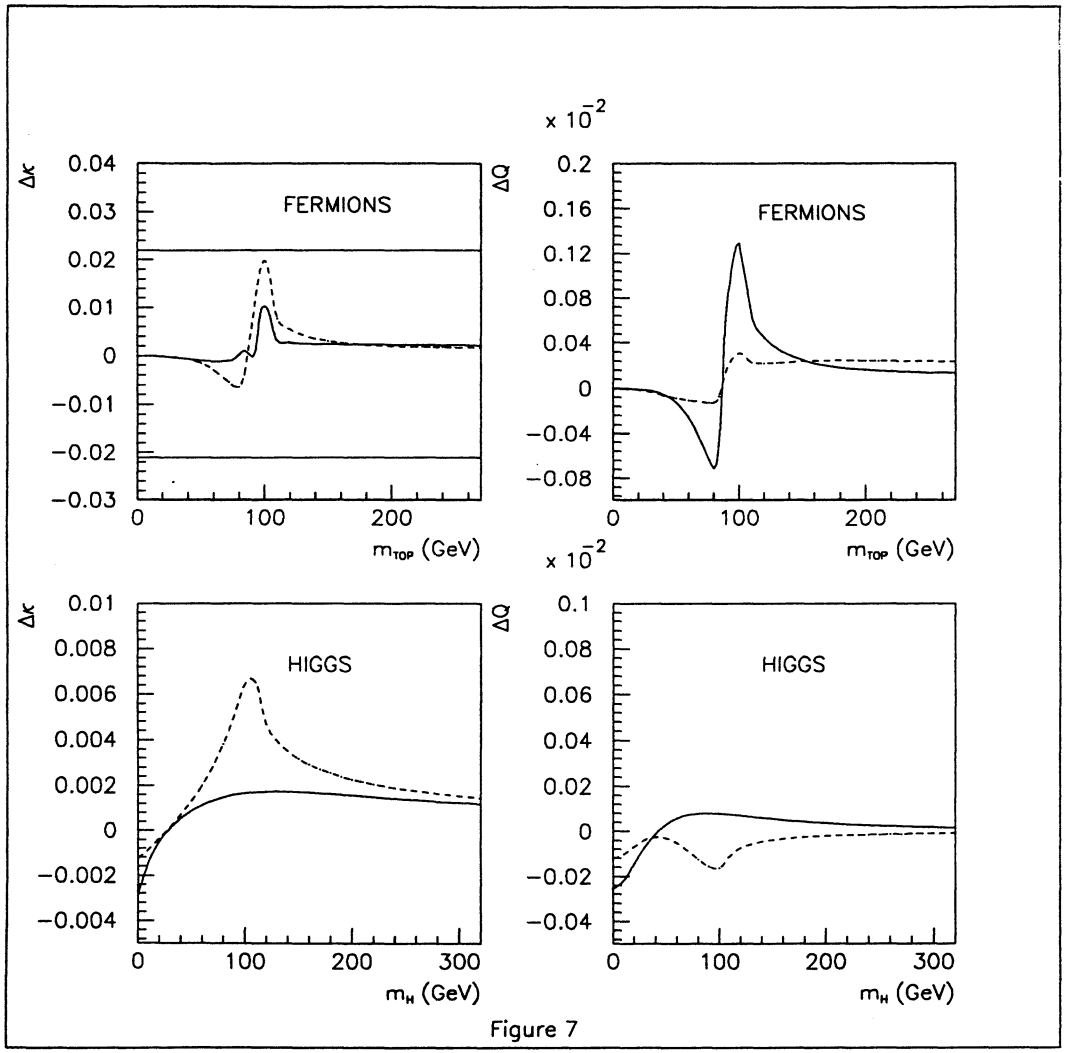

Figure 7

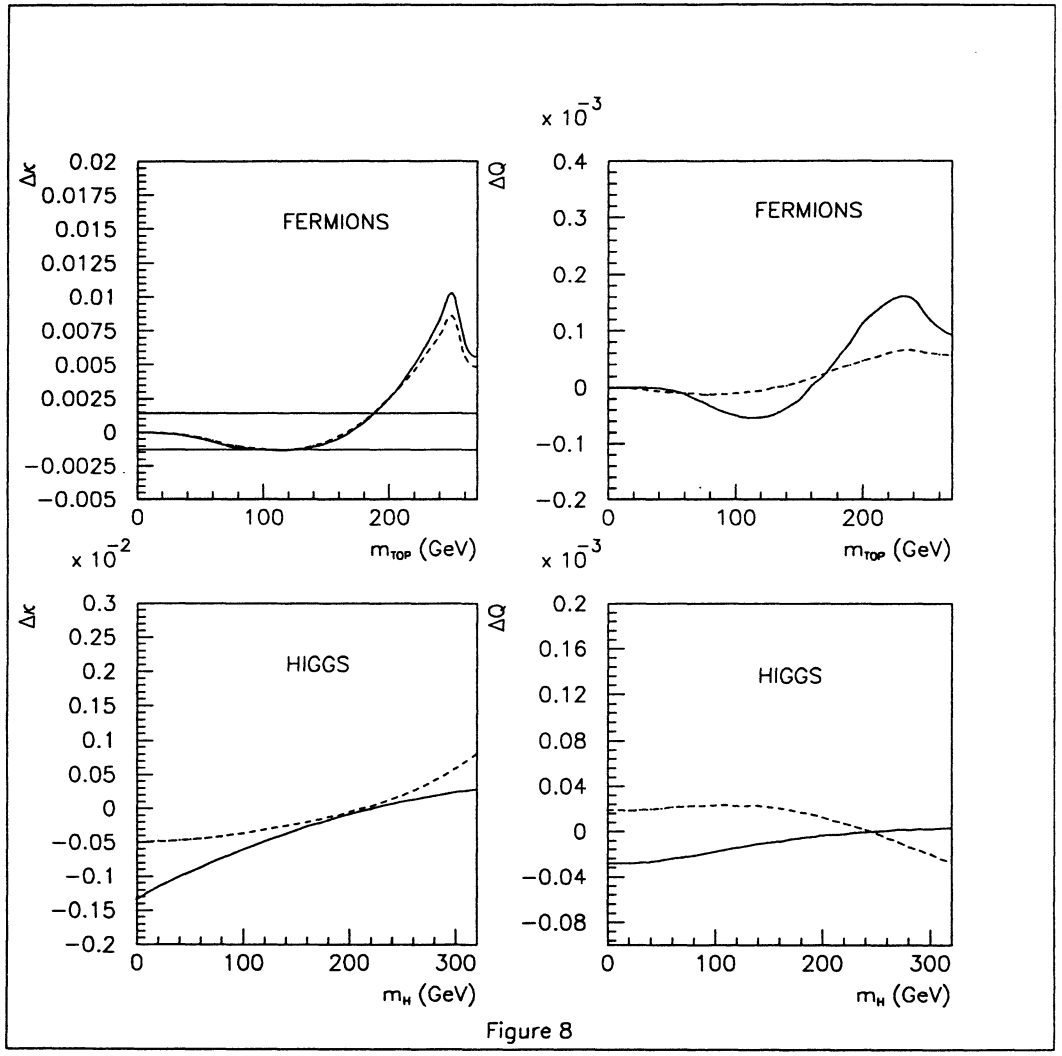

Figure 8